www.claris-eu.org
Deliverables

Instrument: **SP1 Cooperation**

Thematic Priority: **Priority Area 1.1.6.3 "Global Change and Ecosystems"**

FP7 Collaborative Project – Grant Agreement 212492

CLARIS LPB
A Europe-South America Network for Climate Change Assessment and Impact Studies in La Plata Basin

DELIVERABLES

D4.7:WP4 Workshop: Discussions on the impact of SSTs interannual-to-decadal trends and relative role of ocean basins in explaining the observed LPB hydroclimate changes during the 20th century. Discussions on the uncertainties from models agreements in simulating/detecting relevant climate processes underlying observed trends and “shifts” to guide similar works addressing uncertainties in rainfall projection under scenario of climate change.

Due date of deliverable: Month 36

Start date of project: **01/10/2008** Duration: 4 **years**

Organization name of lead contractor for this deliverable: P10-USP

Deliverable No	Deliverable title	WP	Lead beneficiary	Estimated indicative person-months (permanent staff)	Nature	Dissemi nation level	Delive ry date
D4.7	WP4 Workshop: Discussions on the impact of SSTs interannual-to-decadal trends and relative role of ocean basins in explaining the observed LPB hydroclimate changes during the 20th century. Discussions on the uncertainties from models agreements in simulating/detecting relevant climate processes underlying observed trends and "shifts" to guide similar works addressing uncertainties in rainfall projection under scenario of climate change.	WP4	P10-USP	13	R	PU	36

Report

Originally this workshop was to be held on month 36. However, given that WP4 finishes on that month we decided to have an internal workshop to address the objectives a few months before. The meeting was held on May 6th and 7th in Montevideo. The workshop was attended by 10 people from Argentina, Italy and Uruguay. The objective was to present the work to date for deliverables 4.6, and 4.7, as well as to decide the research topics for next and last 5 months of the WP4 in order to finish addressing the WP4 objectives. The meeting consisted in a first day of oral presentations and discussion of the results by all the participants and a second day of exchange of ideas for future work and writing of the reports. We report here on the presentations and discussions during the workshop.

Presentations

1. Sensitivy simulations of South America summer climate to SST changes projected by CMIP3 models – **Carolina Vera (UBA).**
2. LPB hydro-climate variability at interannual and interdecadal timescales as simulated by GCM experiments – **Annalisa Cherchi (CMCC).**
3. Investigating decadal variability in HADCM3 model – **Stefanie Talento (UR).**
4. Land-atmosphere coupling in the El Niño influence over South America – **Marcelo Barreiro (UR).**
5. Maximum and minimum temperature trends over southeast South America from different datasets – **Andrea Carril (UBA).**
6. Large-Scale patterns linked to low-frequency variability of daily intensity of extreme rainfall over argentina – **Federico Robledo (UBA).**
7. Climate change impacts on atmospheric circulation and daily precipitation in the Argentine Pampas region - **Olga Penalba (UBA).**

1) Carolina S. Vera[1], Clementine Junquas[123], L. Li[3], H. Letreut[3]
[1]Centro de Investigaciones del Mar y la Atmosfera/CONICET-UBA (CIMA), and DCAO/FCEyN, Universidad de Buenos Aires, Buenos Aires, Argentina.
[2]Ecole Polytechnique, France
[3]Institute Pierre Simon Laplace (IPSL)/LMD, Paris, France.

Sensitivy simulations of South America summer climate to SST changes projected by CMIP3 models

Previous works have shown that precipitation variability at both tropical and subtropical regions of South America exhibits considerably level of co-variability at a wide range of timescales ranging from synoptic, intraseasonal to interannual. Positive precipitation anomalies over the subtropical plains of La Plata Basin (LPB) region tend to occur in association with negative anomalies over the South Atlantic Convergence Zone (SACZ) region and vice versa. In addition, long-term future climate simulations project in general positive trends in summer precipitation over LPB. The objective of this work is therefore to explore changes in the leading patterns of precipitation year-to-year variability in South America in the context of a climate change induced by GHG increment, and to explore how much of those changes account for the trends projected for the LPB mean summer precipitation.

The leading pattern of precipitation variability (EOF1) was identified by an EOF analysis applied to austral summer rainfall anomalies of CMAP dataset and 18 CMIP3 model outputs for the period 1979-1999. It was found that 16 CMIP3 models are able to represent the EOF1 pattern characterized by a dipolar-like structure with centers of action of opposite sign over the LPB and the SACZ regions, respectively. However, models in general tend to locate the SACZ-related center further northeastward than observed. Similar diagnostic studies are currently being done for the recently available historical simulations of the WCRP/CMIP5 dataset.

EOF1 was also identified for the CMIP3 XXI climate change simulations for SRESA1B scenario over the period 2001-2100. The corresponding time series was used to determine wet and dry active events in southeastern South America. It was found that an increase of the frequency of EOF1 positive events, which means an increase (decrease) of the frequency of wet events in LPB (SACZ) region, is in average projected for the second half of the XXI century by the multi-model ensemble. Such projected change is significantly larger than the inter-model variability for a subset of 9 models that also project positive precipitation trends in the mean summer precipitation conditions in the LPB.

Wet events in the LPB associated to EOF1 activity seems to be promoted in present climate by a differential warming of the equatorial Pacific surface oceanic conditions compared to that in the Atlantic Ocean. The analysis of the results obtained from the CMIP3 XXI century simulations show that such conditions seem to intensify in the context of climate change. It is concluded that the positive trend of austral summer precipitation in LPB projected for the end of the XXI century by most of the CMIP3 CGCMs, seems to be associated with an increase of the frequency of events associated with the leading pattern of year-to-year variability.

Simulations performed with the LMDZ model confirmed that the SST change projected by the WCRP/CMIP3 models induce changes in the climate of South America. Experiments forcing the atmosphere with the zonally averaged SST changes projected by the CMIP3 models by the end of XXI century, showed over South America, a rainfall increase in the tropical band and rainfall decrease in the subtropical regions. On the other hand, numerical experiments performed forcing the atmosphere with the zonal asymmetric signal of the projected SST changes mainly associated with a differential warming of the Indian-Pacific equatorial sector, induces upper-level divergence in the western tropical Pacific, and an intensified subsidence over tropical South America, and particularly in the SACZ region. This change is also associated with a Rossby wave train linking the western tropical Pacific and South America and favouring a rainfall increase over the LPB. Nevertheless, it is worth to point out that these numerical experiments still exhibit large levels of uncertainties considering that the dispersion represented by the 30 members of the ensemble performed with the LMDZ model is important and larger than the projected changes.

2) Annalisa Cherchi, Andrea F. Carril and Laura Zamboni,
Centro Euro-Mediterraneo per i Cambiamenti Climatici/Istituto Nazionale di Geofisica e Vulcanologia

LPB hydro-climate variability at interannual and interdecadal timescales as simulated by GCM experiments

South Eastern South America (SESA) experienced a trend toward increased precipitation throughout most of the last century (e.g. Barros et al., 2008). It is likely that anthropogenic climate forcing may explain part of the wetting trend as IPCC AR4 model simulations predict only a weak increase in SESA precipitation over the last century (Seager et al., 2010). At interannual timescales SESA precipitation has been linked to El Nino Southern Oscillation (ENSO) with a clear seasonality in the connection (Aceituno, 1988; Grimm et al., 2000; Peagle and Mo, 2002; Grimm, 2003; Casez-Boezio et al., 2003; Vera et al., 2006; Barreiro, 2010; among others). The IPCC AR4 models performance in simulating SESA precipitation at seasonal and interannual timescales indicates that they have problems in representing accurately the variability associated with the South Atlantic Convergence Zone, and models having a good ENSO tend to have a good teleconnection in South America (e.g., Silvestri and Vera, 2008; Vera and Silvestri, 2009). For the variability at timescales lower than interannual there are some hypothesis of a possible influence of Pacific decadal variability (Barreiro, 2010), including the role of the 1976/77 North Pacific climate shift (Huang et al., 2005); or of the tropical Atlantic SSTA, as the tropical component of the AMO (Seager et al., 2010). However, clear hypothesis on the mechanisms involved are still missing.

The aim of this analysis is to study the hydro-climate variability over SESA at interannual variability and at lower than interannual timescales, focusing on two main aspects:

- the coupled model performance;
- the identification of the forcing component on the variability even at timescales lower than interannual

Methodology: The model simulations used for the present analysis consists of a 20th century simulation (20c3m) using the INGV-SXG coupled model (Gualdi et al., 2008) that is included in the IPCC AR4 dataset but that has never been included in analysis for this region; and of a set of 9 members AMIP-type simulations using the ECHAM4 GCM (Roeckner et al., 1996) forced with prescribed SST taken from the HadISST dataset (Rayner et al., 2003). The comparison between the two sets of simulation is worth of study as they share the same atmospheric component. The results are compared with land precipitation taken from CRU (Mitchell and Jones, 2005) and atmospheric fields taken from the NCEP reanalysis (Kalnay et al., 1996).

The experiments analyzed show that the model, both in forced and coupled configuration, tends to overestimate the amount of precipitation over SESA but it tends to underestimate its variability in all the seasons considered (JFM, AMJ, JAS and OND). In the AMIP-type experiments the SESA index (identified as the averaged precipitation in the region 37S-19S, 65-47W including land points only) is significantly correlated with CRU data in JAS and OND, suggesting that in these two seasons the role of the forcing from oceanic SST is large. The precipitation and low level wind patterns in correspondence of strong and weak SESA indices (using 1 and -1 standard deviation unit as a threshold) are realistically simulated by the model even if the intensities are weaker than observed. In terms of large-scale connection, the correlation between the SESA index and global SST reveals that in spring SESA precipitation is positively correlated with the tropical Pacific and Indian Oceans, the subtropical Atlantic Ocean and negatively correlated with the North and South extra-tropical Pacific Ocean. The patterns are realistically represented in the AMIP-type experiments but they are weaker in the coupled model simulation. In fact, in this case the correlation with the tropical Pacific is larger toward the western part of the basin rather than the eastern as in the observations; the connection with both the Indian and Atlantic sectors is largely weaker than observed and the connection with the North and South Pacific is missing.

When the SESA index is filtered using a 7-years filter to keep the frequencies lower than 7 years the correlation is still significant and larger in winter and spring. In austral spring, the filtered SESA index correlated with global SST shows that the connection is positive and large in the subtropical south Atlantic, in the north and south subtropical Pacific, in the tropical Indian Oceans, while it is negative in the extra-tropical north Pacific. In the AMIP-type experiments the regions of teleconnections are realistically captured but in the coupled model experiment the correlation is realistic in the western Pacific and in the subtropical south Atlantic, even if weaker than observed, but it is missing in the Indian and extra-tropical Pacific basins.

The dominant modes of variability of the precipitation over South America in OND are characterized by a north-south dipole with centers at 15S and 30S in the eastern part of the continent as first mode (fig. 1a), with the PC1 representing the variability related to ENSO, a triple with centers at 5S, 20S and 35S as second mode (fig. 1b) with the associated PC2 representing a variability at decadal timescales and by an east-west dipole with centers between 15-20S as third mode (fig. 1c) and an associated PC3 representing a trend. The model is able to realistically represent the EOF patterns both in AMIP-type (fig. 1d,e,f) and coupled configuration (fig. 1g,h,i), but it is weaker in capturing the correct time variability. When the PCs are correlated with global SST, in the first mode it is possible to indentify the patterns related to ENSO. In the coupled model the pattern is realistic in the tropical sector, even for the Atlantic Ocean, but not in the extra-tropics. In particular the model misses the right connection between ENSO and the north Pacific as it is wrongly triggered by model biases and air-sea coupling influences (Cherchi et al., 2011). For both PC2 and PC3 it is hard to identify a correspondence between the model simulations and the observations, this is a further indication of the model, and of the coupled model in particular, difficulty in capturing variability at frequency lower than interannual.

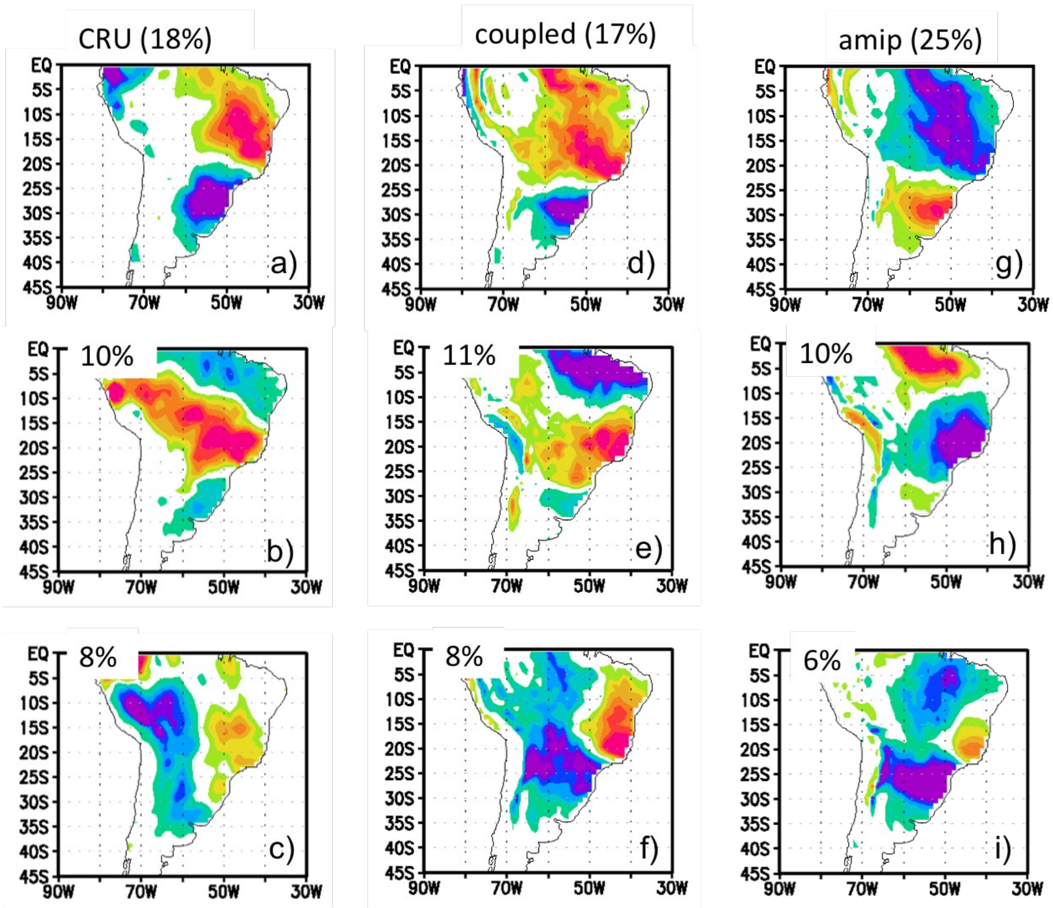

Figure 1 - 1st, 2nd and 3rd EOFs (from top to bottom) patterns of South America precipitation averaged in OND for CRU dataset (a, b, c), for the coupled model experiment (d, e, f) and for the AMIP-type simulations (g, h, i).

The Southern Annual Mode (SAM) influences as well the variability of precipitation over SESA (Thompson and Wallace, 2000). Following, Vera and Silvestri (2009) a SAM index is defined here as the difference of zonal mean geopotential height at 500 mb between 40S and 65S. The relationship between SESA precipitation and SAM has changed during the 20th century (Silvestri and Vera, 2009). In the coupled model the simulation of SAM is not realistic, and it tends to show the typical errors of the CMIP3 coupled models (Vera and Silvestri, 2009) except for JAS where the centers of action are well captured. The changes in the connection between SESA index and SAM during the last decades are shown in fig. 2 as a 19 years sliding correlation between the two indices. In particular, in spring and fall the correlation becomes significant and negative after the mid-70s, in summer there is no significant correlation and in winter the correlation is significant and positive after the 70s (fig. 2a). The set of AMIP-type simulations shows a change to a negative and significant correlation after mid-70s during spring (fig. 2b), suggesting that the change should contain a component that is forced by the SST, while in the other seasons the performance is weaker implying a larger role of the internal variability. In the coupled model experiment, the correlation is not significant in OND and JFM, but it shows some interesting changes in JAS and AMJ (fig. 2c).

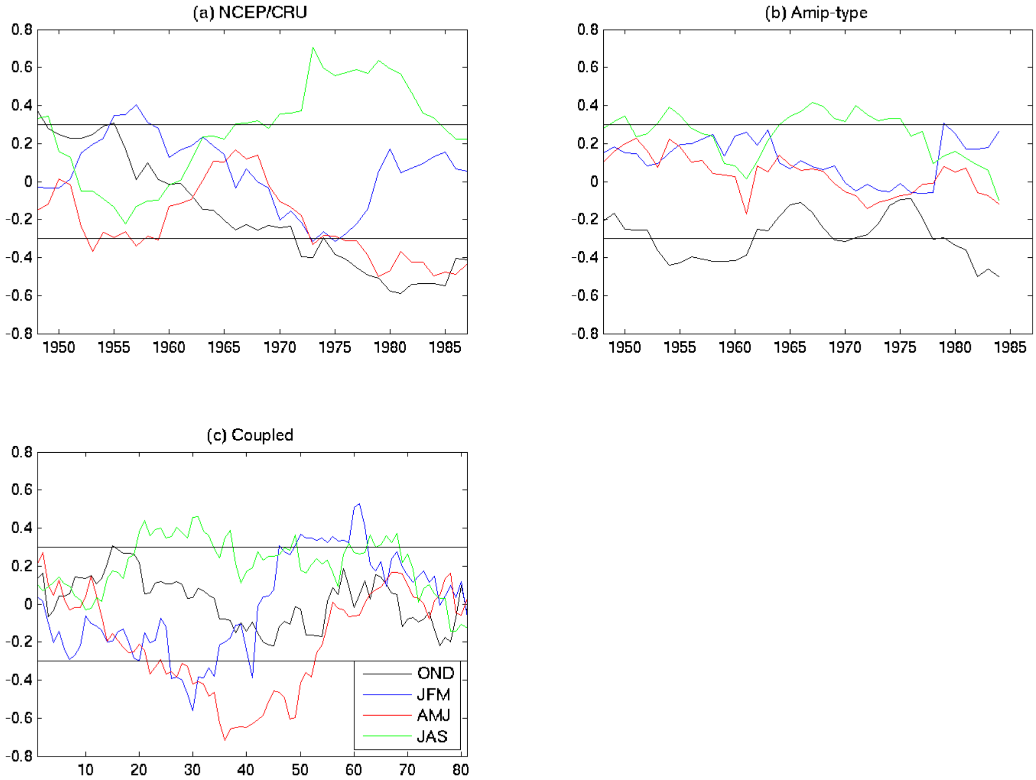

Figure 2 - 19-years sliding correlation between SAM index and SESA precipitation index during the seasons indicated in the legend for (a) the NCEP/CRU datasets, (b) the AMIP-type simulations and (c) the coupled model experiment.

References:

Aceituno P (1988) On the functioning of the Southern Oscillation in the South American sector. Part I: Surface climate. Mon Wea Rev, 116, 505-524.

Barreiro M (2010) Influence of ENSO and the South Atlantic Ocean on climate predictability over southeastern South America. Clim Dyn, DOI:10.1007/s00382-009-0666-9.

Barros VR, Doyle ME, Camilloni IA (2008) Precipitation trends in southeastern South America: Relationship with ENSO phases and with low-level circulation. Theor Appl Climatol, 93, 19-33.

Casez-Boezio G, Robertson AW, Mechoso CR (2003) Seasonal dependence of ENSO teleconnections over South America and relationships with precipitation in Uruguay. J Climate, 16, 1159-1176.

Cherchi A, Masina S, Navarra A (2011) Tropical Pacific – North Pacific teleconnection in a coupled GCM: Remote and local processes. Accepted on International Journal of Climatology.

Grimm A (2003) The El Nino impact on the summer monsoon in Brazil: Regional processes versus remote influences. J Climate, 16, 263-280.

Grimm A, Barros VR, Doyle ME (2000) Climate variability in southern South America associated with

El Nino and La Nina events. J Climate, 13, 35-58.
Gualdi S, Scoccimarro E, Navarra A (2008) Changes in tropical cyclone activity due to global warming: results from a high-resolution coupled general circulation model. J Clim, 21, 5204–5228
Huang HP, Seager R, Kushnir Y (2005) The 1976/77 transition in precipitation over the Americas and the influence of tropical sea surface temperature. Clim Dyn, 24, 721-740.
Kalnay E and co-authors (1996) The NCEP/NCAR 40-year reanalysis project. Bull Am Meteor Soc, 77, 437-471.
Mitchell and Jones (2005) An improved method of constructing a database of monthly climate observations and associated high-resolution grids. Int. J. Climatology, 25, 693-712, DOI: 10.1002/joc.1181.
Paegle JN, Mo KC (2002) Linkages between summer rainfall variability over South America and sea surface temperature anomalies. J Climate, 15, 1389-1407.
Rayner NA, Parker DE, Horton EB, Folland CK, Alexander LV, Rowell DP, Kent EC, Kaplan A (2003) Global analysis of sea surface temperature, sea ice and night marine air temperature since the late nineteenth century. J Geophys Res 18(D14): 4407. doi:10.1029/2002JD002670
Roeckner E, Arpe K, Bengtsson L, Christoph M, Claussen M, Dumenil L, Esch M, Giorgetta M, Schlese U, Schulzweida U (1996) The Atmospheric general circulation Model ECHAM4: Model description and simulation of present-day climate. Max-Planck Institut fu¨r Meteorologie, Report no. 218, Hamburg, p 86
Seager R, Naik N, Baethgen W, Robertson A, Kushnir Y, Nakamura J, Jurburg S (2010) Tropical oceanic causes of interannual to multidecadal precipitation variability in Southeast South America over the past century. J Climate, 23, 5517-5539.
Silvestri G, Vera C (2009) Nonstationarity impacts of the Southern Annular Mode on Southern Hemisphere climate. J Climate, 22, 6142-6148.
Silvestri G, Vera C (2008) Evaluation of the WCRP-CMIP3 model simulations in the La Plata basin. Met Appl, 15, 497-502.
Vera C, Silvestri G (2009) Precipitation interannual variability in South America from the WCRP-CMIP3 multi-model dataset. Clim Dyn, 32, 1003-1014.
Vera C, Silvestri G, Liebmann B, Gonzalez P (2006) Climate change scenarios for seasonal precipitation in South America from the IPCC AR4 models. Geophys Res Lett, 33, L13707, DOI:10.1029/2006GL025759.

3) Stefanie Talento[1], Marcelo Barreiro[2] and Gabriel Cazes-Boezio[1]
[1] IMFIA, Universidad de la República
[2] Unidad de Ciencias de la Atmósfera, Universidad de la República

Interdecadal variability in the HadCM3 model

The objective is to quantify and validate the natural decadal variability of processes relevant to La Plata Basin's climate in the HadCM3 coupled model. With this aim we select 4 time series representative of La Plata Basin's climate variability and analyse their variability both in model simulations and in observations.

We have three different simulations of the HadCM3 model: the pre-industrial, the 20th century and the future scenario A1B run. By definition, all the variability encountered in the preindustrial run is natural variability. On the other hand the 20th century and future scenario runs may also contain forced variability. To validate the model variability in the 4 time series selected we compare the 20th century variability with the observed variability computed from the available observations (in this case: the NCEP-NCAR reanalysis and Reynolds Sea Surface Temperature).

The 4 time series selected are: the first 3 inter-annual principal components (pc1, pc2 and pc3) of regional precipitation (in the region between 50ºS-10ºN and 280ºE-330ºE) and the Pacific Decadal Oscillation Index (PDO, defined as the leading inter-annual principal component of the sea surface temperature in the Pacific Ocean poleward of 20ºN).

In order to make a fair comparison of the time series variabilities across the different types of simulations we define a standard pattern of variability (the pattern obtained in the 20th century run) and project all the simulations onto this standard pattern to obtain the desired principal component. As an example, if eof1 is the first eof of regional precipitation in the 20th century run we obtain the pre-industrial pc1 projecting the pre-industrial precipitation field onto eof1. We perform the principal component analysis for every quarter of the year.

There are several measures to quantify the variability of a time series. The simplest one is to compute the standard deviation, that can be seen as computing the deviation of the series from a 0-order polynomial. To complement this measure, and to account for possible trends in the data sets, we also compute deviations from a 1-order and 4-order polynomial.

For the pc1 the results show that the variability of the HadCM3 in the present-climate simulation is comparable with the observed variability, although the simulated variability is considerably higher than the observed one during summer season. According to a F-test with 95% confidence level, and measured as deviations form a 0-order polynomial, the pc1 variability in the future scenario is higher than the 20th century variability in every quarter of the year form July-August-September to January-February-March. On the other hand, measured as deviations form 1-order or 4-order polynomials the results remain the same only for July-August-September and August-September-October.

For pc2 and pc3 no statistically significant differences are found in the variabilities neither between the three model simulations nor with the observed analogues with any of the measures described above.

The PDO exhibits similar variability in the 20^{th} run and in the observations. Again, according to a F-test with 95% confidence level, and measured as deviations form a 0-order polynomial, its variability is higher in the sresA1B scenario than in the 20^{th} century in every quarter of the year.

Finally, in order to better analyse decadal variability, we applied a low-pass filter to all the 4 time series and repeated the calculations. For a 5 years low-pass filter the main results indicate that the decadal variability of the pc1 is higher in the future scenario than in the 20th century, with a 95% confidence level, in every quarter of the year (in every quarter of the year excepting September-October-November) considering deviations form a 0-order (1-order) polynomial.

4) Marcelo Barreiro and Nicolas Díaz
Unidad de Ciencias de la Atmósfera, Universidad de la República, Uruguay

Land-atmosphere coupling in El Niño influence over South America

Climate variability in South America is influenced by El Niño with strong dependence on the season and region considered (e.g. Ropelewski and Halpert, 1987). The atmospheric bridges that connect the equatorial Pacific with South America have been studied in detail for several decades and the main mechanisms are well understood (e.g. Grimm and Ambrizzi, 2009). That is, however, not the whole story because once the signal arrives over a certain continental region the atmospheric anomalies will be modified by the interaction with the surface, a process that only recently has received attention (Koster et al., 2004). Tropical areas during summertime are clear candidates for having a strong coupling between land and the overlying atmosphere, because it depends on the exchanges of energy and water in the boundary layer that will affect the development of clouds, precipitation and the atmospheric circulation. Using atmospheric models, it has been shown recently that South America is a region where the interaction between soil moisture and precipitation is important to correctly simulate the climatological fields and the South American Monsoon (e.g. Xue et al., 2006). In this study we investigate the role of the interaction between soil moisture and the atmosphere in setting up the climate anomalies over South America induced by El Niño. We concentrate in the austral summer and beginning of fall, that is, in the decay phase of El Niño. The effects of La Niña during summer are less clear than those of El Niño and will not be considered here.

The study shows that during summer and the beginning of fall the influence of El Niño over South America is controlled by the interaction between the soil moisture and the overlying atmosphere. This is particularly true for the surface air temperature anomalies, which acquire the right sign only if the model includes the land-atmosphere coupling (compare Figures 1, 2 and 3). The structure and sign of the precipitation anomalies are less affected, but the amplitude increases particularly over SESA. As result, with interactive soil moisture the model is able to capture the warm-dry and cold-wet relationships that are observed in northern South America and SESA, respectively. While the precipitation anomalies associated with El Niño during summertime in South America were reported before, the findings of this study show for the first time a cooling signal over SESA mainly due to a decrease in the maximum temperature, which is consistent with the physical arguments used above to explain the wet-cold relationship.

These results have clear consequences for the seasonal forecasts of temperature and precipitation because while the pattern of precipitation anomalies are mainly dependent on the large scale atmospheric anomalies associated with El Niño and thus a model that represents the atmospheric teleconnections correctly will tend to locate the anomalies in the right place with the correct sign, the amplitude of precipitation anomalies, as well as the pattern and sign of surface temperature anomalies are controlled not only by the large scale atmospheric circulation, but also by the local interaction between the soil moisture and the atmospheric anomalies. These same processes may be operating at longer timescales and might partially explain the observed trends in rainfall and surface temperature in the LPB.

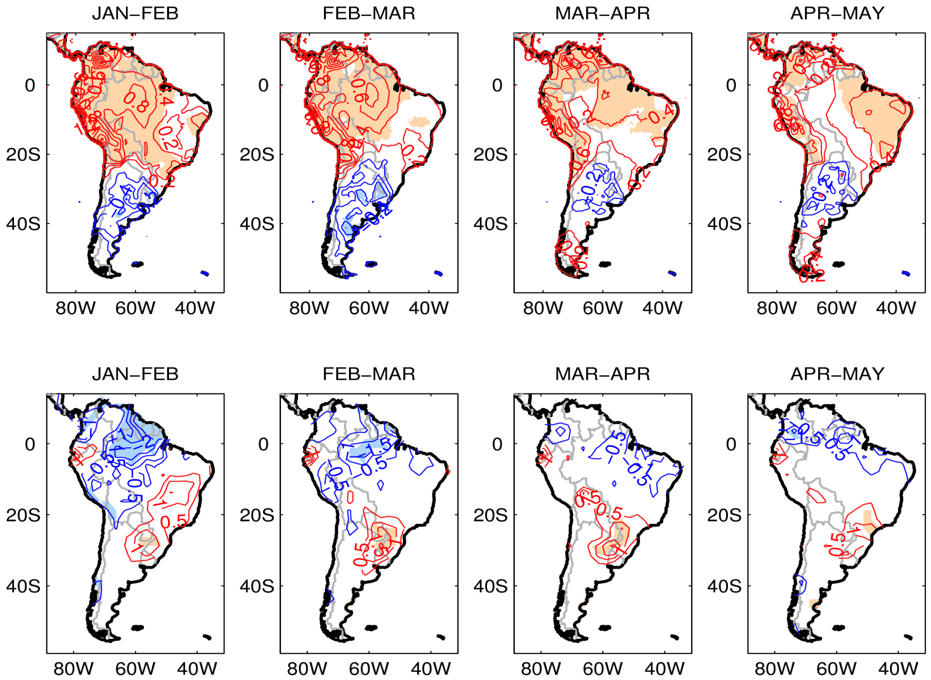

Figure 1- Observed surface air temperature (above) and precipitation (below) anomalies during El Niño

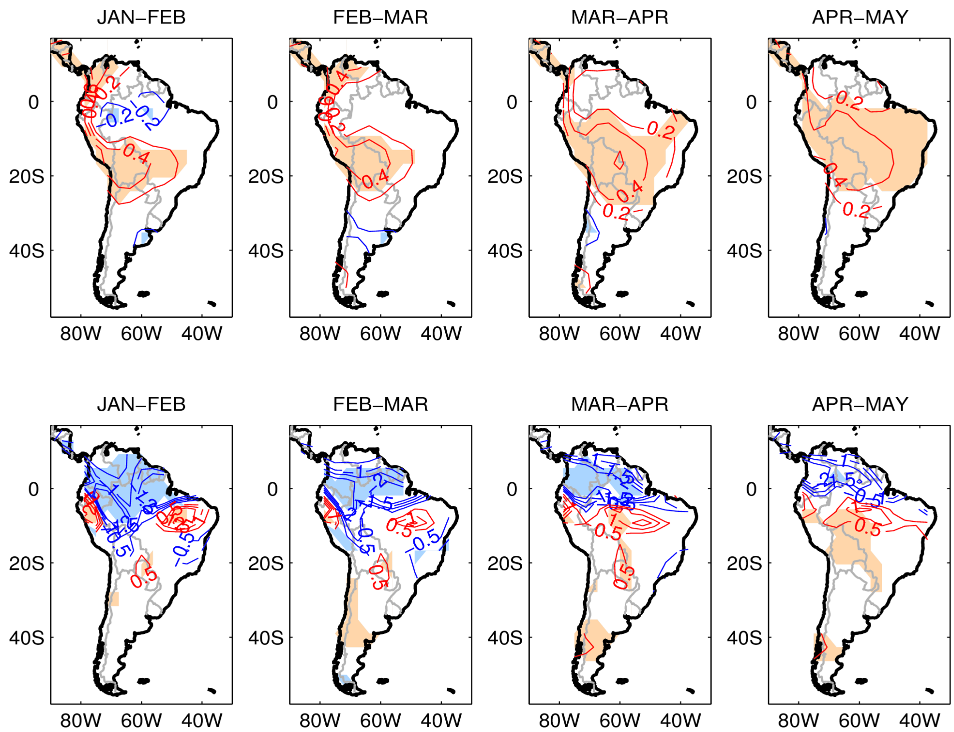

Figure 2 – Same as Figure 1 but for a model without land-atmosphere coupling.

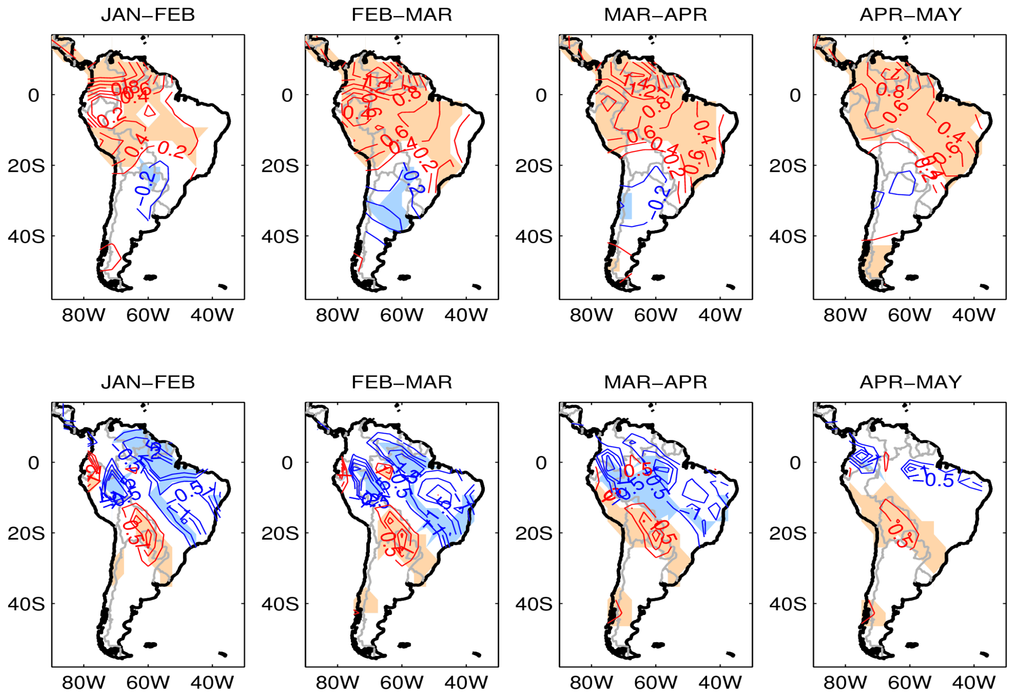

Figure 3 – Same as figure 1 but for a model with land-atmosphere coupling.

References

Grimm AM, Ambrizzi T. 2009. Teleconnections into South America from the tropics and extratropics on interannual and intraseasonal time scales, *in Past Climate Variability in South America and surrounding regions: from the Last Glacial Maximumto the Holocene, Developments in Paleoenvironmental Research and Risk Assessment*, edited by F. Vimeux et al., pp. 159-191 doi:10.1007/978-90-481-2672-9.

Koster RD et al. 2004. Regions of Strong Coupling Between Soil Moisture and Precipitation. *Science* **305**: 1138-1140.

Ropelewski CH, Halpert S. 1987. Global and regional scales precipitation patterns associated with El Niño-Southern Oscillation. *Monthly Weather Review* ***115***: 1606-1626.

Xue Y, De Sales F, Li W, Mechoso CR, Nobre C, Juang H-MH. 2006. Role of land surface processes in South American monsoon development. *Journal of Climate* **19**: 741–762

CLARIS | LPB

CLARIS | LPB

A Europe-South America Network for Climate Change Assessment
And Impact studies in La Plata Basin

SEVENTH FRAMEWORK PROGRAMME

www.claris-eu.org
Deliverables

5) Pablo Zaninelli[1], Andrea F. Carril[1], Claudio G. Menéndez[1], Annalisa Cherchi[2], Laura Zamboni[2]
[1] *Centro de Investigaciones del Mar y la Atmósfera/CONICET-UBA, Argentina.*
[2] *Centro Euro-Mediterraneo per i Cambiamenti Climatici/Istituto Nazionale di Geofisica e Vulcanologia*
Cross-WP6-WP4 activities.

Part I: Maximum and minimum temperature trends over southeast south America from different data sets.

A number of datasets are commonly used by the scientific community with climate analisis purposes: analysis generated by the major forecasting centers, and gridded datasets developed by different group of research. The objective of this work is to verify if the available gridded datasets of near surface temperature over southeast South America (SESA) give us confidence on detecting trends in daily extremes temperatures. Trends in maximum surface temperature (TX) and minimum surface temperature (TN) are estimated using the following datasets: NCEP-1, 20CR, ERA-40 and Tencer. The NCEP/NCAR Reanalysis 1 project (Kalnay et al. 1996) is an analysis/forecast system used to perform data assimilation of the past data (from 1948 to the present). Data are available in a global grid, every 6 hours at about 2.5°. The 20th Century Reanalysis Project (20CR, Compo et al. 2011), is an effort to produce a reanalysis spanning the entire twentieth century, but assimilating only surface observations of synoptic pressure, monthly sea surface temperature and sea ice distribution. 20CR is a 6-hourly, 4-dimensional global atmospheric dataset spanning 1871 to present, intending to place the atmospheric circulation patterns into a historical perspective. The re-analysis project ERA-40 (Uppala et al. 2005) covers the period from mid-1957 to mid-2002, overlapping the earlier re-analysis (ERA-15) from 1979 to 1993. ERA-40 datasets are based on quantities analysed/forecasted using the ERA-40 data assimilation/forecasts scheme, and are with 6-hours frequency in a 1° global grid. Tencer et al. (2011) is a novel gridded dataset of maximum and minimum temperatures spanning over the period 1960-2000, and covering the domain 70°W-45°W and 40°S-20°S (see Figure 1). ERA interim (Berrisford et al. 2009) and NCEP-2 (Kanamitsu et al. 2002) were not considered due to the short period in which they span.

Definition of extremes is based on a percentile approach (P75 and P25; see Table I). Although other authors have defined more restrictive thresholds (e.g., Vincent et al. 2005 is based on P10 and P90; Rusticucci and Barrucand 2004 have used P5 and P95), we adopt the criteria by Carril et al. (2008) looking for enhance the signals.

P75 in TX	Warm days
P25 in TX	Cold days
P75 in TN	Warm nights
P25 in TN	Cold nights

Table I: Definition of extremes

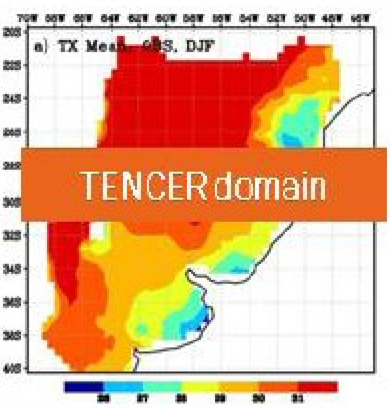

Figure 1: Domain considered

Mean percentile fields used to define warm days and cold nights are displayed in Figure 2 (period of the analysis is 1961-2000). Spatial patterns of ERA-40 percentiles compares well with those

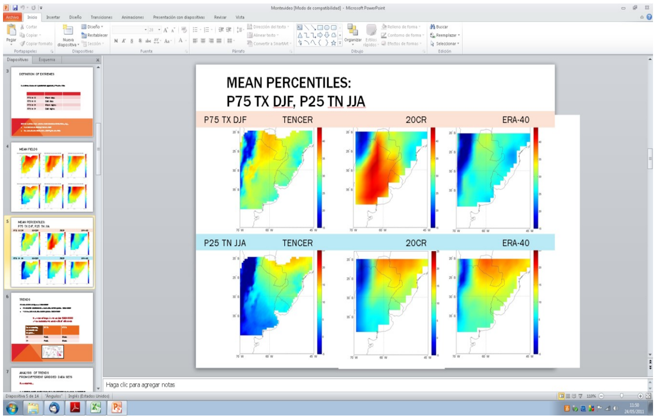

Figure 2 - Percentile 75th (25th) in TX (TN) for summer (winter) in different datasets.

from Tencer, although ERA is somewhat cooler than Tencer in summer. Main uncertainties arrive from 20CR in summer, when P75 in TX maximizes over central Argentina. We also highlight the dispersion among the climatologies over the Andes region, partially due to the low resolution of the models and differences in the representation of the topography.

To evaluate trends in extreme near surface fields, reference period is 1961-1980. Trends are evaluated as the number of days in the period 1981-2000 exceeding the percentile of the reference period. First, we estimate the trends month by month, as the number of days exceeding a daily percentile with a 5-day window (percentile approach as in Vincent et al. 2005). Then we repeat the month by month analysis, changing the window for the percentile estimation (from 5 to 30-day window). The results are summarized in tables of phase agreement/disagreement over the Tencer region as illustrated in Figure 3. For the moment, this was done following a subjective appreciation: Tencer is the reference climatology and yellow (red) boxes indicate that a particular dataset presents trends in phase (not in phase) with those from Tencer. Table II summarizes the results in terms of phase agreement.

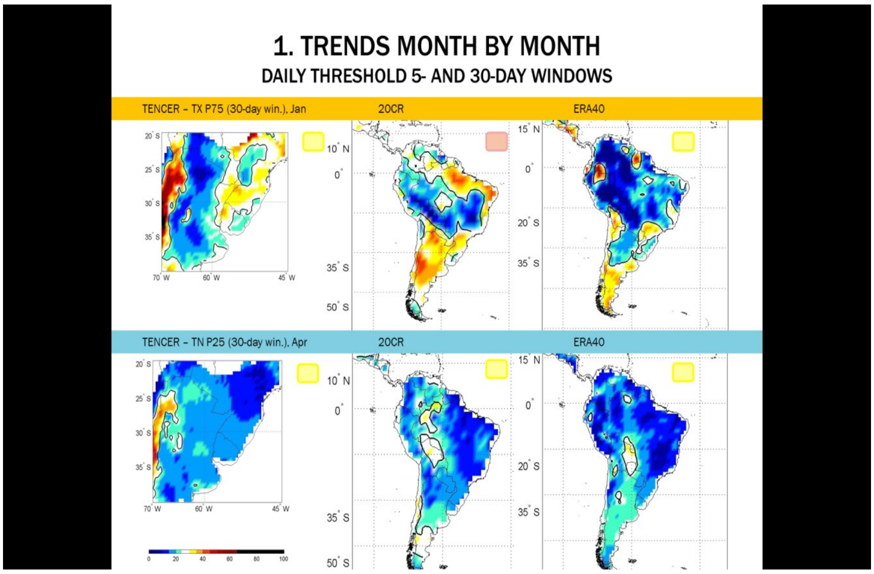

Figure 3 - Agreement or disagreement criteria

As it is displayed in Table II, there are a number of cases in which sign of trends disagrees (red boxes), some cases in which trends from different datasets has coincident sign (yellow boxes) and other cases in which trends are only partially in phase (white boxes). It is hard to conclude about the sensitivity test to the window used to define the percentile of reference (5-day vs. 30-dat window): in some cases some improvements are found when finer scales are considering but in other cases agreements appears when removing the higher frequencies. We are now processing the NCEP-1 data to be included in the present analysis. Moreover, we are designing an objective method to quantify agreements/disagreements among the datasets.

TX P75 - LPB REGION
The period of the analysis is 1980-2000
Reference threshold is the percentile of a previous period (1960-1979)

TX P75	5-day window				30-day window		
Month	TENCER	20CR	ERA40	Month	TENCER	20CR	ERA40
Jan				Jan			improved
Feb				Feb			improved
Mar			improved	Mar			
Apr			improved	Apr			
May				May			
Jun				Jun		improved	improved
Jul				Jul		improved	improved
Aug				Aug			
Sept				Sept			
Oct				Oct			
Nov				Nov			
Dec				Dec			

TN P75 - LPB REGION
The period of the analysis is 1980-2000
Reference threshold is the percentile of a previous period (1960-1979)

TN P75	5-day window				30-day window		
Month	TENCER	20CR	ERA40	Month	TENCER	20CR	ERA40
Jan				Jan		improved	
Feb				Feb			
Mar				Mar			
Apr				Apr		improved	improved
May				May		improved	improved
Jun				Jun			
Jul				Jul			
Aug				Aug			
Sept				Sept		improved	improved
Oct				Oct			improved
Nov				Nov		improved	
Dec				Dec			improved

TX P25 - LPB REGION
The period of the analysis is 1980-2000
Reference threshold is the percentile of a previous period (1960-1979)

TX P25	5-day window				30-day window		
Month	TENCER	20CR	ERA40	Month	TENCER	20CR	ERA40
Jan				Jan			
Feb				Feb			
Mar				Mar			
Apr			improved	Apr			
May				May			
Jun				Jun			
Jul				Jul		improved	
Aug		improved		Aug			
Sept				Sept			
Oct				Oct			
Nov				Nov			
Dec				Dec			

TN P25 - LPB REGION
The period of the analysis is 1980-2000
Reference threshold is the percentile of a previous period (1960-1979)

TN P25	5-day window				30-day window		
Month	TENCER	20CR	ERA40	Month	TENCER	20CR	ERA40
Jan				Jan			
Feb				Feb		improved	
Mar				Mar		improved	improved
Apr				Apr			
May				May			
Jun				Jun		improved	
Jul				Jul		improved	
Aug				Aug		improved	
Sept				Sept			improved
Oct				Oct			improved
Nov				Nov		improved	
Dec				Dec			

Table II: Tables of agreement/disagreement to reproduce trend in near surface temperature extremes. Left (right) panels are for TX (TN) in summer (winter).

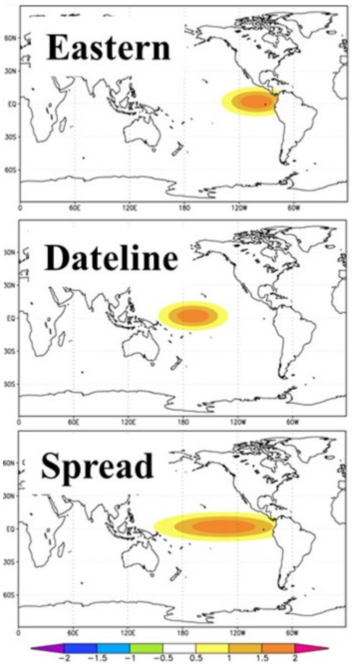

Figure 4 - Idealized forcing

Part II: Links between tropical Pacific SST anomalies and temperature extremes over south America.

A control run and a set of six sensitivity experiments to idealized anomalies in the tropical Pacific SST were conducted at CMCC, integrating ECHAM4 AGCM at T106 resolution. The control run is a30-year length experiment forced with climatological SST. The sensitivity experiments, 30-year length each one, were forced with climatological SST everywhere, except in the tropical Pacific where an idealized anomaly is superimposed. The anomalies superimposed respond to an idealized ENSO in the eastern basin, in the dateline region or spread between both regions (see figure 4). Three of those experiments were forced with a positive (El Niño-like) superimposed anomaly while in the other three the superimposed anomaly is La Niña-like (negative anomaly). Superimposed anomalies are only turned on during October-November, in order to simulate the ENSO onset.

Those experiments now are being used to study the potential links between the occurrence of anomalies in the tropical Pacific sector and the occurrence of extremes over South America. It is a work on progress.

References

Berrisford et al., 2009: The ERA-Interim archive – Version 1.0, ERA reports

Carril et al., 2008: Heatwaves in Europe: Areas of homogeneous variability and links with the regional to large-scale atmospheric and SSTs anomalies, Clim. Dyn., 30, 77-98, DOI: 10.1007/s00382-007-0274-5

Compo et al., 2011: The Twentieth Century Reanalysis Project. Quart. J. Roy. Met. Soc., 137: 1–28. DOI:10.1002/qj.776

Kalnay et al., 1996: The NCEP/NCAR 40-year reanalysis project. Bull. Amer. Meteor. Soc., 77, 437-470.

Kanamitsu et al., 2002: NCEP–DOE AMIP-II REANALYSIS (R-2). Bull. Amer. Meteor. Soc., 1631-1643. DOI: 10.1175/BAMS-83-11-1631

Rusticucci and Barrucand, 2004: Observed Trends and Changes in Temperature Extremes over Argentina. J. Clim, Notes and Correspondence, 17, 4099-4107

Uppala et al., 2005: The ERA-40 re-analysis. Q. J. R. Meteorol. Soc., 131, 2961-3012.

Tencer et al., 2011: A Southeastern South American daily gridded data set of observed surface minimum and maximum temperature for 1991-2000. Bull. Amer. Meteor. Soc., submitted.

Vincent et al., 2005: Observed Trends in Indices of Daily Temperature Extremes in South America 1960–2000. J. Climate, 18, 5011-5023

*6) Federico A. Robledo [1, 2 *]; Olga C. Penalba [1] and Carolina Vera[1, 3]*
[1] Departamento de Ciencias de la Atmósfera y los Océanos. FCEN-UBA. Buenos Aires Argentina
[2] Consejo Nacional de Investigaciones Científicas y Técnicas, CONICET. Buenos Aires, Argentina
[3]Centro de Investigaciones del Mar y de la Atmósfera. CONICET/UBA Buenos Aires, Argentina

Large-Scale Patterns Linked To Low-Frequency Variability Of Daily Intensity Of Extreme Rainfall Over Argentina

The main goal of this work is to analyzed planetary and regional features of the atmospheric circulation that impact in the extreme rainfall on Argentina. The analysis has been made on the basis of the leading pattern of covariabilty between spring the daily intensity of extreme rainfall (DIER) in Argentina and sea surface temperature (SST) for all the oceans from 17.5º N to 90º S.

This analysis was performed using a Singular Values Decomposition (SVD) for spring in the period 1962 to 2005. Two data sets were used to the SVD analysis: monthly SST from the Kaplan SST V2 from the NCEP/NCAR and high quality daily rainfall for 35 surface stations from the National Weather Service of Argentina distributed throughout the country. The monthly mean of daily intensity of extreme rainfall index (DIER) is the quotient between the monthly accumulated extreme rainfall (AE) and the number of days with extreme precipitation events per month (PE). We consider extreme daily precipitation when rainfall is greater than the mean 75th daily percentile for the period 1961 to 2000. Regression maps between SVD times series and relevant variables like meridional wind and streamfunction at 200 hPa, SST and DIER were performed in order to describe leading patterns signal on the southern hemisphere circulation.

The three leading SVD modes of the coupled SST and DIER variations account around 72 percent for spring of the total square covariance (TSC). The first mode of spring explains 45% of TSC. Spatial pattern of the leading mode are associated with SST anomalies resembling those typically linked to ENSO with 4-year temporal cycles and enhanced DIER in central and eastern Argentina. Regression maps of circulation anomalies depict Rossby-like wave trains emanating from central tropical Pacific and equatorial Indian oceans, in a similar way than those previously identified by other papers as promoted by ENSO events (Figure 1).

The second SVD mode that explains 17% of TSC, presents an anomalous cooling in the tropical Atlantic Ocean as well as in the Indonesian Sea associated with low DIER over northeastern Argentina. This mode shows a significant decadal variability with two sub-periods: 8 years and 12 years. An upper-level cyclonic circulation anomaly is observed southward of the negative SST anomaly center located over the equatorial Atlantic. On the other hand, an anticyclonic circulation is identified over southeastern South America. Both features seem to be part of a Rossby-like wave train extending from western tropical Pacific Ocean arching toward South America. Evidences of an annular circulation structure are also observed over the Polar Regions in association with this particular SVD mode (Figure 2).

The third SVD mode explains 10% of TSC and shows significant variability on periods around 14 years. A horseshoe-like shape characterizes the SST anomalies over the western Pacific related with this SVD mode while negative (positive) DIER extends over northern (central-east) Argentina. Circulation anomalies extend between New Zealand region and South America in relation to the third SVD mode (Figure 3).

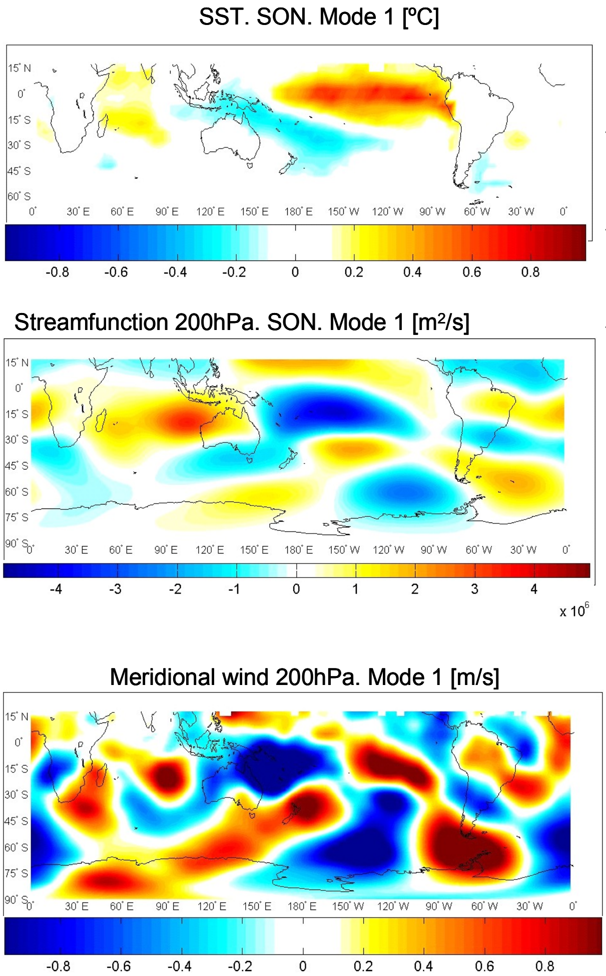

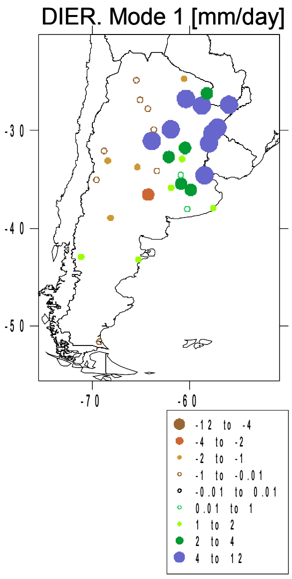

Figure 1. Regression maps between SVD times series of SST and relevant anomalies of variables: SST (top, left), DIER (top, right), streamfunction (middle) and meridional wind (bottom) at 200 hPa

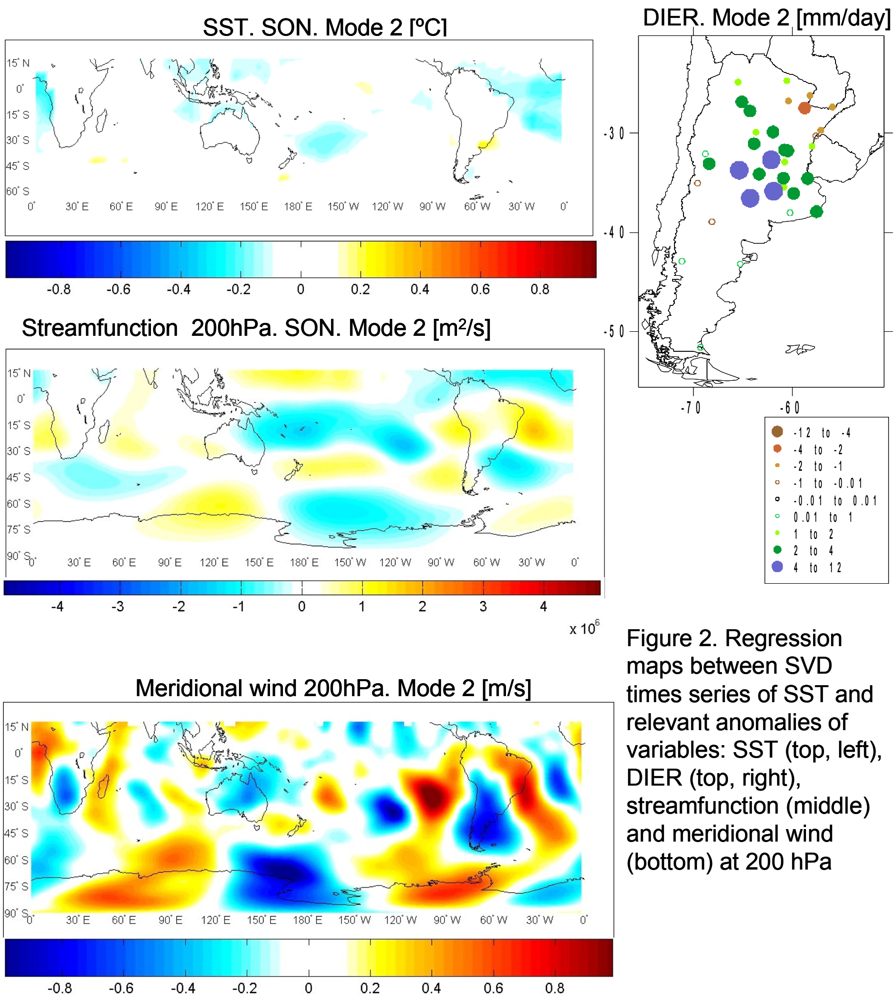

Figure 2. Regression maps between SVD times series of SST and relevant anomalies of variables: SST (top, left), DIER (top, right), streamfunction (middle) and meridional wind (bottom) at 200 hPa

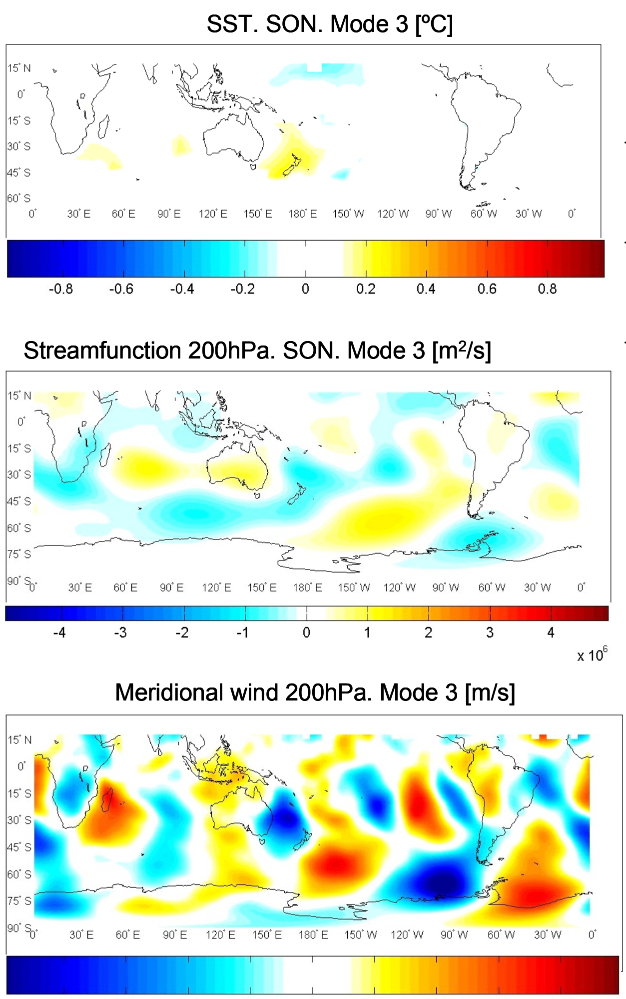

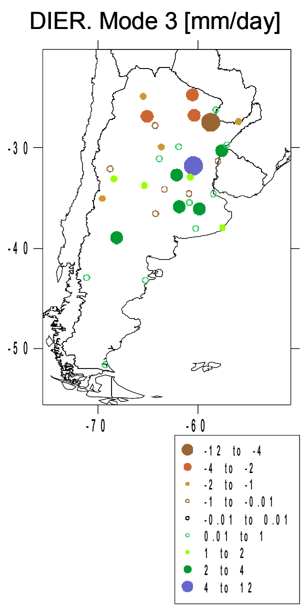

Figure 3. Regression maps between SVD times series of SST and relevant anomalies of variables: SST (top, left), DIER (top, right), streamfunction (middle) and meridional wind (bottom) at 200 hPa

7) Olga C. Penalba [1] - M. Laura Bettolli [1,2]
[1] *Departamento de Ciencias de la Atmósfera y los Océanos, FCEN, Universidad de Buenos Aires, Argentina*
[2] *Consejo Nacional de Investigaciones Científicas y Técnicas, Argentina*

Climate change impacts on atmospheric circulation and daily precipitation in the Argentine Pampas region

The skill of the General Circulation Models (GCMs) in representing the circulation that conducts or conditions the precipitation events has an important role in the evaluation of future climate projections. However, the capacity of the GCMs in representing the circulation on a synoptic scale has been little explored yet. The usefulness of the GCMs in local studies is restricted by their poor spatial resolution. Techniques of scale reduction have been developed as bridges between the large scale information generated by the GCMs and the local scale information, with the purpose of performing short- to midrange forecasts and to study the potential impacts of future climate change. In this way, the use of daily results from the GCMs for studies of local climate is subject to their aptitude in representing the atmospheric systems on a regional scale.

In this context, the present work is structured to fulfill the following objectives: to characterize the rainfall conditions and their probability of occurrence in the Pampas region; to identify daily circulation patterns in southern South America and to associate them with different rainfall conditions in the Pampas region; to evaluate the representation of the daily circulation patterns as simulated by a set of 12 GCMs; and to analyze the projected changes of the same patterns at different time horizons of the 21th century.

Different data-sets were used in this study: **a)** Daily mean sea level pressure (SLP) fields corresponding to the NCEP reanalysis 2 were used as representative of observed circulation for the period 1979-1999. The chosen domain extends from 15ºS to 60ºS and from 42.5ºW to 90º W on a 2.5º latitude-longitude grid. **b)** Daily rainfall series located in the Argentine Pampas region, provided by the Argentine National Meteorological Service. **c)** GCM outputs from the climate of the 20th century (20C3M) were used to describe present climate and the SRES A1B 720 ppm stabilization experiment were used to represent future climate (2010-2040, 2046-2065 and 2081-2100). The set of 12 GCMs analyzed outputs is available at the Program for Climate Model Diagnosis and Intercomparison (PCDMI) and from the ENSEMBLES CERA archives. The analysis focuses on winter (JJA) and summer (DJF).

Cluster analysis was performed coupled with PCA to determine the NCEP dominant circulation patterns. The resulting classification has five and seven circulation type categories for summer and winter, respectively. For each CT, the spatial structures, the relative frequency, the transitions between pairs of CTs, and the persistence, were analyzed. Then a comparative analysis between NCEP and the GCMs was performed.

Summer dry days are related to the most persistent circulation type, corresponding to an intensification of the southern Atlantic anticyclone, which interrupts the passage of the eastern perturbations and diverts them to the south (CT4s). Rainy days are significantly benefited by patterns that could be related to a post-frontal intense anticyclone that induces east-southeast anomalous flow and moisture advection over the region (CT1s). Heavy rainy days are significantly related with a cyclonic disturbance at the centre of the continent associated with a cold front passage (CT2s).

Winter dry days are significantly favored by a high pressure system that extends from the Atlantic

Ocean to the centre of the continent (CT4w). Rainy days and heavy rainy days are significantly benefited by structures with a high pressure system at the south of the continent, enhancing an anomalous flow from the east-southeast to the central region of Argentina and a corresponding moisture advection at low levels (CT5w).

The climatic characteristics of the mean SLP patterns show a notorious seasonality. This seasonality is of great importance in determining the low-level circulation and its associated moisture advection in the region. These principal climatic characteristics of the atmospheric circulation of summer and winter are reasonably well captured by the GCMs, although the seasonality is exaggerated. For example, during winter, the Westerlies are displaced towards the equator, attenuating the contribution of the subtropical highs. During summer, both semi-permanent high systems more extended to the south than the observed fields. Most models tend to show a lower contribution of the mean pattern in comparison to NCEP and, therefore, a higher presence of perturbations.

With respect to the circulation types (CTs), the models are able to reproduce the full range of summer and winter circulation types found in the NCEP climatology. For present climate, an inter-model variability of the representation of the summer patterns is observed. The GCMs estimate reasonably well the frequency of atmospheric situations that favor summer dry days (CT4s, Figure 1 a). For the two future time horizons analyzed, a trend of reduction of the circulation patterns associated with dry days and an increment of the frequencies of the patterns associated with rainfall of the region is observed (CT4s and CT2s, Figure 1 b and c). This is in agreement with other climate change studies over the region that shows positive trends in the total seasonal precipitation and changes in the precipitation variability during summer.

Contrary to what is observed for summer, during winter the GCMs estimate reasonably well the frequency of the circulation types, especially those that favor heavy rain and dry conditions over the region (CT5w, Figure 1 a). The majority of the GCMs indicate an increment of these patterns for future climate, principally during the second half of the 21th century (Figure 1 b and c).

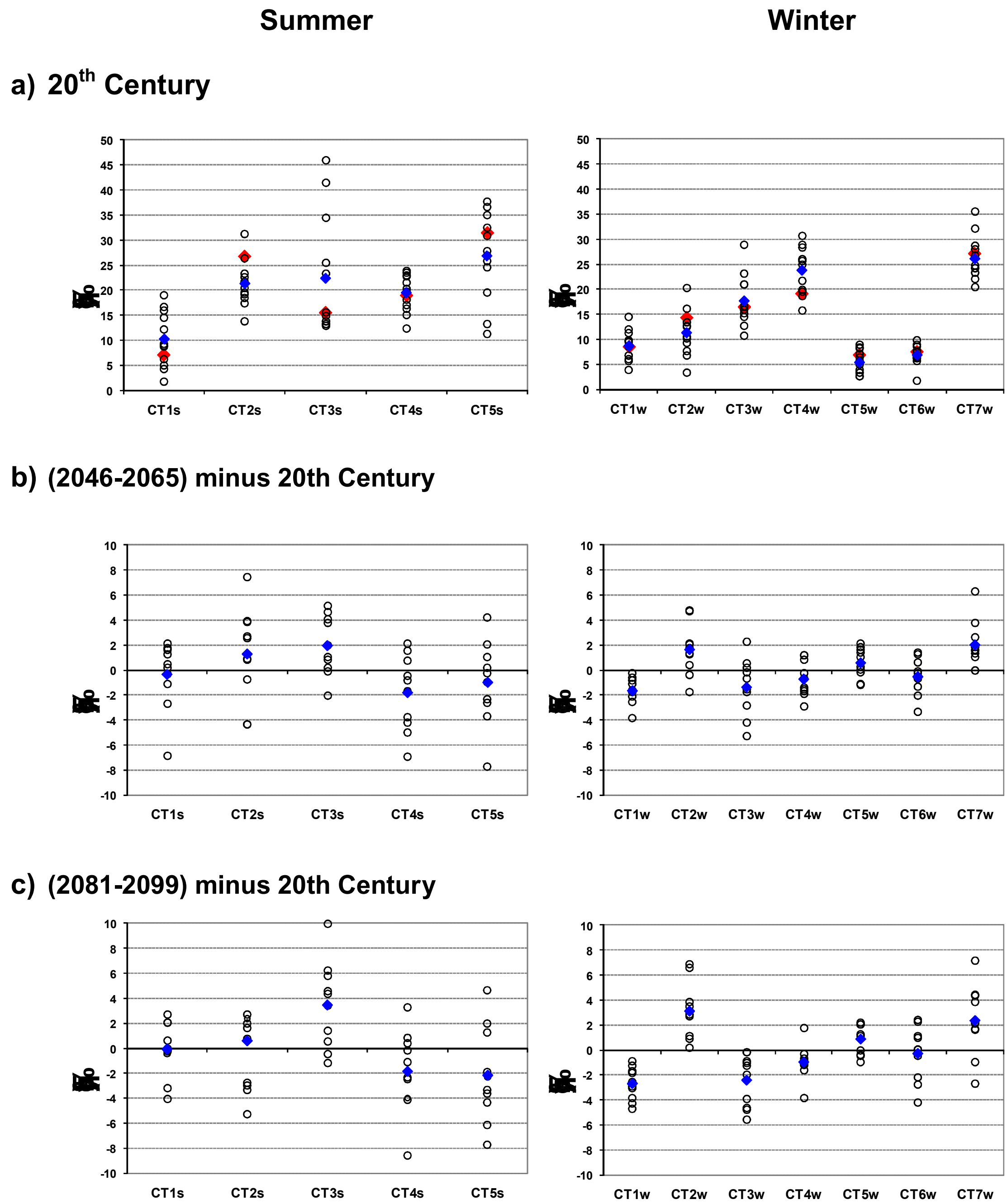

Figure 1 - Frequency (%) of circulation types for summer and winter for NCEP (red diamond), GCMs (circles) and ensemble of GCMs (blue diamond) for the 20th Century (a). Future changes of the frequencies of the CTs for the period 2046-2065 (b) and 2081-2099 (c).